3 Generation of mid-infrared pulses by $\chi^{(3)}$ difference frequency generation in CaF_2 and BaF_2

Tunable mid-IR pulses in the range 1300–4200 cm^{-1} (7.7–2.4 μm) are generated through a phase-matched four-wave mixing process in ordinary mid-IR window materials such as calcium fluoride and barium fluoride. In this process, the difference frequency $\omega_3 = 2\omega_2 - \omega_1$ is generated from pump fields ω_1 and ω_2. The process can be phase-matched to different frequencies by adjustment of the angle between the pump fields.

3.1 Introduction

The common methods for generating femtosecond mid-infrared pulses employ various kinds of three-wave mixing processes, such as difference frequency generation and optical parametric generation and/or amplification (OPG/OPA), which is used for all pump–probe experiments in this thesis. As explained in §2.1, these processes all rely on the second-order polarization $P^{(2)}(t) \propto \chi^{(2)}E^2(t)$ created by a high-intensity field $E(t)$. This second-order polarization is nonzero only in materials that lack inversion symmetry. Then, fields with (angular) frequencies ω_1 and ω_2 couple to a field with frequency $\omega_3 = \omega_1 \pm \omega_2$. A high efficiency can only be obtained if the phase-matching condition $\mathbf{k}_3 = \mathbf{k}_1 \pm \mathbf{k}_2$ is fulfilled. The wavevectors $\mathbf{k}_x$ have magnitudes $k_x = \omega_x/n_x$, where n_x is the index of refraction at frequency ω_x. Since in a medium with a normal dispersion, $n(\omega)$ is a monotoneously increasing function of ω, the phase-matching condition is usually achieved by employing the birefringence of the $\chi^{(2)}$ material. The polarizations of the different fields are then chosen such that the ω_3 field experiences a lower index of refraction than the ω_2 field. In order to be suitable for $\chi^{(2)}$ infrared generation, a crystal should (1) be transparent for the wavelengths involved, (2) lack inversion symmetry, and (3) be sufficiently birefringent. There are many crystalline materials that satisfy these requirements for wavelengths shorter than 4.5 μm, such as BBO, KTP, potassium titanyl arsenate (KTA), $LiNbO_3$, and $KNbO_3$. However, for many molecular vibrations other than the OH stretch, such as the CO stretch in organic molecules, longer wavelengths are necessary. Unfortunately, the available crystals for wavelengths beyond 4.5 μm, such as $AgGaS_2$,[48] GaSe,[56] and $ZnGeP_2$[98] cannot be directly pumped with the currently available high-intensity 800 nm Ti:sapphire lasers.

As an alternative to the $\chi^{(2)}$-based pulse generation discussed above, we will now consider $\chi^{(3)}$ (or four-wave-mixing) processes. Here, three fields interact and drive a third-order polarization $P^{(3)}(t) \propto \chi^{(3)}E^3(t)$. Compared to $\chi^{(2)}$ processes, the advantage of $\chi^{(3)}$ processes is that $\chi^{(3)}$ is nonzero in any medium, without any restrictions on the crystal symmetry. Therefore, $\chi^{(3)}$ frequency mixing is, in principle, possible in any medium, in-

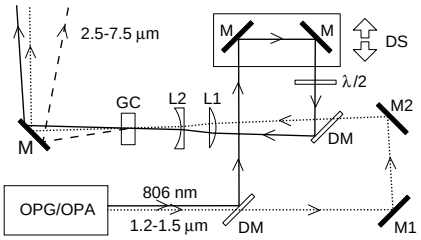

FIGURE 3.1. Setup for $\chi^{(3)}$ pulse generation. Abbreviations: OPG/OPA: optical parametric generation/amplification infrared source; DM: dichroic mirror; M, M1, M2: mirrors; $\lambda/2$: half-wave plate; DS: delay stage; L1, L2: 2:1 telescope (BK7 glass); GC: generation crystal (4 mm CaF_2 or BaF_2). We used M1 and M2 to adjust the angle between the pump and the signal beams.

cluding isotropic media. Since the latter have no birefringence, one must use alternative means to fulfill the requirement of phase-matching.

Pulses in various wavelength ranges have been generated by means of $\chi^{(3)}$ techniques. For example, far-infrared (around 60 cm^{-1}) pulses have been generated in air.[18] Due to the low value of $\chi^{(3)}$ in air, the pulse energy was only about 5 pJ, which required time-gated and phase-sensitive THz detection schemes. In the ultra-violet, the properties of certain modes in hollow fibres have been employed to generate light in gases at well-chosen pressures with $\sim 4\,\mu$J pulse energies.[24] Further, in the mid-infrared, 1064 nm and tunable dye-laser pulses have been combined to generate tunable picosecond pulses at $\sim$1 pJ pulse energies in a phase-matched $\chi^{(3)}$ process.[93]

In this chapter, we show how the approach of Ref. 93 can be used to generate mid-IR (2.4–7.6 μm) pulses with high energies and femtosecond durations with the currently available titanium-sapphire laser systems. Here, pump fields with frequencies ω_1 and ω_2 generate a difference frequency $\omega_3 = 2\omega_2 - \omega_1$, with $\mathbf{k}_3 = 2\mathbf{k}_2 - \mathbf{k}_1$ as the phase-matching condition. We use the common window materials CaF_2 and BaF_2 as generating media. In these non-birefringent materials, phase-matching is possible, despite the fact that they have a normal dispersion. The reason is that the fields $2\omega_2$ and ω_1 are equivalent to the fields with the high and medium frequencies, respectively, while $\omega_2 < \omega_1$ counts for the corresponding indices of refraction.

3.2 EXPERIMENT

We used a commercial Ti:sapphire laser (Quantronix Titan; 100 fs, 2.5 mJ pulses, 1 kHz repetition rate) to pump a parametric conversion device based on BBO (§2.2.2). From the output of the device, we used the signal (6250–8300 cm^{-1}, 300 μJ) and the remaining pump (12400 cm^{-1}, 1.1 mJ) for the ω_2 and ω_1 fields, respectively, as shown in Fig. 3.1. After having been split and recombined for time-overlap, the pulses were collimated to a diameter of approximately 2 mm before interacting in a 4-mm-thick CaF_2 or BaF_2 plate. Because of the properties of the $\chi^{(3)}$ tensor, the intensity of the generated ω_3 field is 9 times higher for parallel ω_1 and ω_2 pump fields than for perpendicular pump fields.[109] Therefore, we used a wave plate to make the polarizations of the pump and signal pulses parallel.

A delay stage enabled adjustment of the time overlap between the pump and signal pulses. At time overlap, we generated pulses with typical energies of 100–200 nJ.

If the laser pulses are focused in air in a collinear geometry, similar to Ref. 18, a measurable amount of infrared is generated as well, but with a typical energy of only 3 nJ and

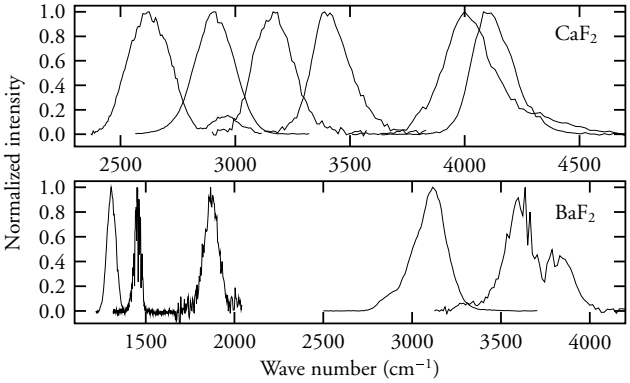

FIGURE 3.2. Typical spectra of the generated pulses in CaF_2 (top) and BaF_2 (bottom). The structure in the spectra at 1500 and 3700 cm^{-1} is caused by absorption lines of water vapor (see also Fig. 1.2).

a bandwidth of 400 cm^{-1} FWHM. Also, a visible amount of light at frequency $2\omega_1 - \omega_2$ is generated in that case.

3.3 RESULTS

Figure 3.2 shows typical spectra of the pulses generated in CaF_2 and BaF_2. We obtained these spectra with a scanning monochromator and PbSe (for the CaF_2 data) and HgCdTe (for BaF_2) detectors. We chose these detectors for their different spectral responses. In order to tune ω_3, we adjusted both ω_2 (defines the difference frequency ω_3) and the angle between $\mathbf{k}_1$ and $\mathbf{k}_2$ (phase-matching). The FWHM bandwidth of the generated spectra is about 200 cm^{-1} for CaF_2 and 40–300 cm^{-1} for BaF_2, respectively. The maximum frequency ω_3 is approximately 4100 cm^{-1}, limited by ω_2, which could not be tuned higher than about 8250 cm^{-1} in our OPG/OPA.

Figure 3.3 shows an autocorrelate for pulses generated in CaF_2 at 2580 cm^{-1}. We measured this by generating the second harmonic of the infrared pulses in a $LiIO_4$ ($\theta =$ 20 deg) crystal. The FWHM autocorrelate width is 298 fs, which corresponds to a 211 fs pulse duration if we assume a Gaussian pulse shape. With a bandwidth of 200 cm^{-1} FWHM, this pulse duration implies $\Delta\nu\Delta\tau = 1.3$ for the frequency–bandwidth product.

Figure 3.4 shows the tuning curve with the generated frequency ω_3 versus the angle $\beta = \angle(\mathbf{k}_1, \mathbf{k}_3)$. Calculated tuning curves are shown as well; we obtain these by substituting $k_x = n_x\omega_x$ in the phase-matching condition $\mathbf{k}_3 = 2\mathbf{k}_2 - \mathbf{k}_1$, which yields

$$\cos(\beta) = \frac{4n_2^2\omega_2^2 - n_1^2\omega_1^2 - n_3^2\omega_3^2}{2n_1n_3\omega_1\omega_3}, \tag{3.1}$$

where n_i are the indexes of refraction as calculated from the Sellmeier equations for CaF_2[58,80] and BaF_2.[58,81] Due to the dispersive properties of these materials, Eq. (3.1) imposes a lower limit on the frequency ω_3 that can be generated in this process. This cut-off occurs at $\beta = 0$ deg.

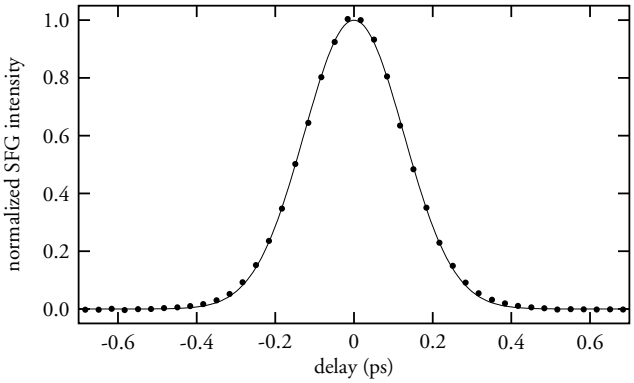

FIGURE 3.3. Autocorrelate of pulses generated in CaF_2 at 2580 cm^{-1} with a fit to a Gaussian pulse shape.

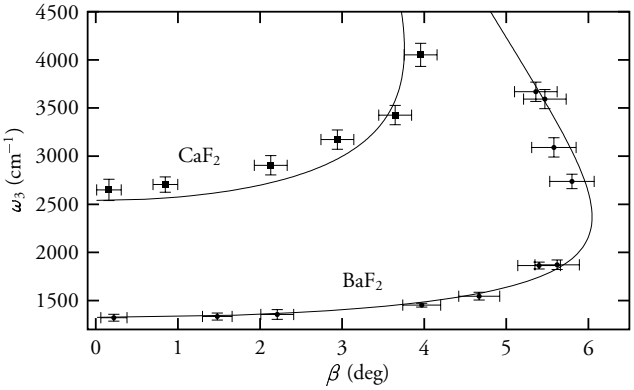

FIGURE 3.4. Tuning curves for BaF_2 and CaF_2. Data points: experiment with the FWHM bandwidth as the vertical errorbar. Drawn lines: calculated tuning curve for $\omega_1 = 12400$ cm^{-1}.

For BaF_2, we obtained a better agreement between experiment and calculated tuning curve if we increased the index of refraction at frequency ω_1 by 1.0×10^{-4}. Instead of 1286 cm^{-1} (7.8 μm) and 6.5 deg for the cut-off frequency and maximum angle, respectively, this yields 1325 cm^{-1} and 6.0 deg, respectively (as shown in Fig. 3.4). In CaF_2, the difference between experiment and theory can result from a frequency-dependent deviation less than 10^{-4} in the refractive index for the ω_2 field. We note that experimental values of the index of refraction are known to differ by similar amounts from the calculated values.[58,80,81]

3.4 Conclusions

We have shown that a $\chi^{(3)}$ difference frequency generation process with two pump fields can be phase-matched in the common infrared window materials CaF_2 and BaF_2, which have no special birefringent or crystal symmetry properties. An 806 nm laser pulse as the high-frequency (ω_1) pump enables the generation of difference frequencies over the range 2.4–7.6 μm with the angle between the pumping fields as a tuning parameter. We obtained pulse energies up to 200 nJ.

As a final note we would like to point out that the presented type of $\chi^{(3)}$ difference frequency generation can be phase matched in *any* material with a normal dispersion relation, although the angles and cut-off wavelengths vary. A common material especially worth mentioning in this respect is NaCl, with $\omega_3 > 600$ cm^{-1} and $\beta < 17$ deg.